Progress In Electromagnetics Research, PIER 54, 303–319, 2005

A UNIQUE SOLUTION TO THE 2-D H-SCATTERING PROBLEM FOR A SEMICIRCULAR TROUGH IN A PEC GROUND PLANE

A. G. Tyzhnenko

Department of Mathematics
Kharkiv National Economic University
Prospect Lenina 9A, 61059, Kharkiv, Ukraine

Abstract—A rigorous solution to the Neumann boundary value problem (BVP) for semicircular trough in a perfectly electrically conducting (PEC) ground plane is presented. The known Rayleigh's method expansion of a solution by eigensolutions of the Helmholtz equation in cylindrical coordinates coupled with partial orthogonality of trigonometric functions is used. In contrast to previous works on this theme, a Fredholm 2nd kind matrix equation for modal coefficients is obtained, which permits one to derive very fast convergent approximate solution for any incidence angle and trough dimension. The method solution permits one to consider a dielectric loading as well. A strong broadband fall-off of backscattering from apertures loaded with lossy dielectric is theoretically revealed.

1. INTRODUCTION

Scattering from a trough in a conducting ground plane is one of the most formidable problems in computational electromagnetics (CEM) if we want to obtain a unique solution to the Helmholtz equation that satisfies both the boundary condition on the whole infinite interface and Sommerfeld condition. The first and widely used method, the generalized network formulation proposed by Harrington and Mautz [1], is relatively simple to compute and implement, but it suffers from the problem of spurious resonances at eigenfrequences of indentation [2]. Theoretically, a unique solution to this problem can be obtained making use of the electric field integral equation (EFIE) or the magnetic field integral equation (MFIE) on the whole infinite interface. However, any numerical realization of such methods needs for truncation of integral equation's domain that, in turn, leads to inadequacy of a numerical solution, which increases with grazing angle diminishing. To weaken this inadequacy, one needs to enlarge the flat pieces from both sides of a roughness. This one leads to dramatic increasing in computational burden. To avoid this, one can apply resistive cards, as in [3], or some version of resistive tapering, as in [4]. Such simulations are very useful in CEM, but they need for testing with the aid of some rigorous method. As such a test method, one could use a solution for scattering from semicircular trough. Many authors treated this problem. In [5–7], this one has been reduced to a 1st kind integral equation. In [8, 9], both the Rayleigh's method expansion of a solution by eigensolutions of the Helmholtz equation in cylindrical coordinates and partial orthogonality of trigonometric functions has been used. However, authors do not overcome the ill-posedness of matrix equation obtained and then their solution, as well as all others obtained in [5–7], may be correct in the low-frequency range only. The most general case of EM wave scattering by dielectric-loaded slots and semicircular troughs with the aid of singular integro-integrodifferential equations has been considered in [10]. The range of correctness of numerical solution of such equations was not specified in the cited paper, other than the numerical results exhibited can be regarded to the low-frequency case only. In [11], an analytic solution to the mentioned problem has been obtained in the low-frequency case as well.

A rigorous solution to this BVP for the TE case (transverse electric to the plane of incidence) was obtained by the author in [12]. In this work, as in [8, 9], the Rayleigh's method coupled with partial orthogonality of trigonometric functions was used. However, in contrast to [8, 9], the additional equation found for modal coefficients permits one to obtain a Fredholm 2nd kind matrix equation for Fourier coefficients, which in turn permits one to obtain a convergent numerical solution for any scatterer size and incidence angle.

In this paper, see also [13], the analogous method is applied for solving the TM scattering problem. A Fredholm 2nd kind matrix equation for Fourier coefficients is also obtained, which yields a unique solution to the mentioned BVP for any grazing angle and scatterer size. An approximate solution of truncated matrix equation converges exponentially fast to an exact solution with truncation number increasing. This issue permits one to obtain an approximate solution with preset accuracy in a very economical way. The simple algorithm obtained permits one to consider a set of semicircular troughs loaded with dielectric cylinders of any dimensions of them in contrast to those considered in [14] for low-frequency case only.

Summarizing, one can define the obtained solution as "semi-analytical": that in which the discretization of the domain is not used but, in contrast to purely analytical procedure, for obtaining an approximate solution one have to solve a Fredholm matrix equation.

The paper is organized as follows. In Section 2, the main principles of the solution are described. In Section 3, the numerical features are given. In Section 4, some numerical results are presented. Here, the comparison with the solution in [7, 9] for TM case is done for the low-frequency case and good agreement is demonstrated. Besides, loading of mentioned trough with lossy dielectric is considered and strong fall-off of backscattering is theoretically revealed for some losses. This fall-off we find for all investigated magnitudes of electric size of the trough ($ka \leq 100$).

2. TM-SCATTERING PROBLEM SOLVING

Consider a problem of H-scattering from a dielectric-loaded semicircular trough in a PEC plane, illuminated by a TM-plane wave (transverse magnetic to the plane of incidence), as is shown in Fig. 1. With a suppressed time dependence of $\exp(j\omega t)$, the z-component of incident magnetic field can be written as

$$H_0(\rho, \varphi, t) = e^{-jk\rho\sin(i_0-\varphi)}, \tag{1}$$

where $k = \omega/c$ is a free space wavenumber. An incident angle, i_0, is counted counterclockwise from the positive OY axis. The dielectric constant is considered as any complex quantity, $\varepsilon = \varepsilon' - j\varepsilon''$ ($\varepsilon'' \geq 0$). We assume the total magnetic field in D^- to be consist of the incident,

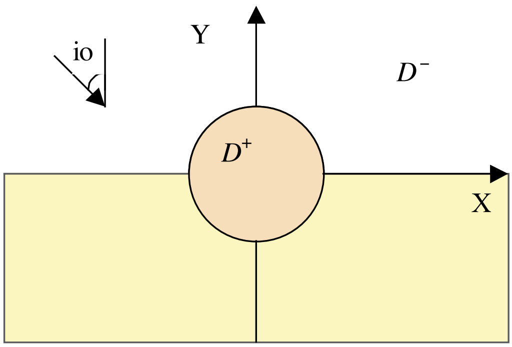

Figure 1. Geometry of the BVP.

reflected, and scattered fields

$$H^-(\rho,\varphi)=e^{-jk\rho\sin(i_0-\varphi)}+e^{-jk\rho\sin(i_0+\varphi)}+\sum_{n=0}^{\infty}a_nH_n^{(2)}(k\rho)\cos n\varphi. \quad (2)$$

The total field in D^+ is represented as

$$H^+(\rho,\varphi)=\sum_{n=1}^{\infty}b_nJ_n(k_1\rho)\sin n\varphi+\sum_{n=0}^{\infty}c_nJ_n(k_1\rho)\cos n\varphi, \quad (3)$$

where $k_1=k\sqrt{\varepsilon_1}$ is the wavenumber inside the dielectric cylinder. The enforcement of the electric and magnetic fields continuity at $\rho=a$ yields the equations

$$\sum_{n=0}^{\infty}a_nH_n\cos n\varphi-\sum_{n=1}^{\infty}b_nJ_n\sin n\varphi-\sum_{n=0}^{\infty}c_nJ_n\cos n\varphi= -e^{-jka\sin(i_0-\varphi)}-e^{-jka\sin(i_0+\varphi)} \quad (4a)$$

$$\sum_{n=0}^{\infty}a_nH'_n\cos n\varphi-\varepsilon_1^{-0.5}\sum_{n=1}^{\infty}b_nJ'_n\sin n\varphi-\varepsilon_1^{-0.5}\sum_{n=0}^{\infty}c_nJ'_n\cos n\varphi= j\sin(i_0-\varphi)e^{-jka\sin(i_0-\varphi)}+j\sin(i_0+\varphi)e^{-jka\sin(i_0+\varphi)} \quad (4b)$$

for $0<\varphi<\pi$, and

$$\sum_{n=1}^{\infty}b_nJ'_n\sin n\varphi+\sum_{n=0}^{\infty}c_nJ'_n\cos n\varphi=0 \quad (4c)$$

for $\pi<\varphi<2\pi$. We use here the following notation for the Bessel functions and their derivatives with respect to the whole argument:

$$H_n=H_n^{(2)}(ka),\quad H'_n=H_n^{(2)\prime}(ka),\quad J_n=J_n(k_1a),\quad J'_n=J'_n(k_1a). \quad (5)$$

Multiplying the equations (4) by $\cos m\varphi$ and integrating both sides with respect to φ upon the corresponding intervals, and using the notation

$$\gamma_{nm} = \begin{cases} 0, & m = n \\ (1-(-1)^{n-m})n/(n^2-m^2), & m \neq n \end{cases},$$

we obtain the following equations for modal coefficients:

$$a_m H_m - \frac{\nu_m}{\pi} \sum_{n=1}^{\infty} b_n J_n \gamma_{nm} - c_m J_m = F_m^{(1)}, \tag{6a}$$

$$a_m H'_m - \frac{\nu_m}{\pi} \varepsilon_1^{-0.5} \sum_{n=1}^{\infty} b_n J'_n \gamma_{nm} - \varepsilon_1^{-0.5} c_m J'_m = F_m^{(2)}, \tag{6b}$$

$$\frac{\nu_m}{\pi} \sum_{n=1}^{\infty} b_n J'_n \gamma_{nm} - c_m J'_m = 0 \tag{6c}$$

with

$$F_m^{(1)} = -2\nu_m j^m \cos m(i_0 + \pi/2) J_m(ka), \tag{7}$$

$$F_m^{(2)} = -2\nu_m j^m \cos m(i_0 + \pi/2) J'_m(ka), \tag{8}$$

and

$$\nu_m = \begin{cases} 1, & m = 0 \\ 2, & m > 0 \end{cases}. \tag{9}$$

Multiplying the equation (4c) by $\sin m\varphi$ and integrating it with respect to φ from π to 2π, we obtain an additional equation that is equivalent to (6c):

$$\frac{2}{\pi} \sum_{n=0}^{\infty} c_n J'_n \gamma_{mn} - b_m J'_m = 0. \tag{10}$$

Note that namely this equation permits one to obtain a well-conditioned system for modal coefficients. In mentioned work [9], the authors solved the equations (6), which yield a very ill-conditioned system after truncating procedure. Condition number of this system increases drastically with truncation order that prevents for obtaining an adequate solution in high-frequency range. Let us prove now that the use of additional equation (10) permits one to obtain a Fredholm 2nd kind matrix equation for modal coefficients. Really, using equations (6b) and (6c), we can obtain the equation without b_n

$$a_m H'_m - 2\varepsilon_1^{-0.5} c_m J'_m = F_m^{(2)}. \tag{11a}$$

Further, deriving $b_m J'_m$ from additional equation (10) and substituting it into (6a), we obtain the second equation without b_n

$$a_m H_m - c_m J_m - \frac{2\nu_m}{\pi^2} \sum_{n=1}^{\infty} \frac{J_n}{J'_n} \sum_{n=0}^{\infty} c_k J'_k \gamma_{nk} = F_m^{(1)}. \tag{11b}$$

We consider here that

$$J'_n = J'_n(k_1 a) \neq 0. \tag{12}$$

It is really so for complex $k_1 a$. Worth noting that condition (12) fulfils for any real rational value of $k_1 a$, other than $J'_n(k_1 a)$ may be very close to zero. However, the ratio J_n/J'_n in (11b) does not approach close to zero that ensures the stability of a solution for any reasonable value of $k_1 a$. We change further the summation order in (11b) supposing the absolute convergence of series. After obtaining the unknowns c_k, we will prove that it is really so. Noting new unknowns

$$\tilde{a}_m = a_m H_m, \quad \tilde{b}_m = b_m J'_m, \quad \tilde{c}_m = c_m J_m, \tag{13}$$

we obtain the following system for only one unknown, $\tilde{c}_k$:

$$\tilde{c}_m + \sum_{k=0}^{\infty} T_{mk} \tilde{c}_k = F_m, \tag{14}$$

where

$$T_{mk} = -\frac{2\nu_m}{\pi^2 \Delta_m} \frac{J'_k}{J_k} \sum_{n=1}^{\infty} \frac{J_n}{J'_n} \gamma_{nk} \gamma_{nm}, \tag{15}$$

$$F_m = \frac{1}{\Delta_m} \left(F_m^{(1)} - \frac{H_m}{H'_m} F_m^{(2)} \right), \tag{16}$$

$$\Delta_m = 2\varepsilon_1^{-0.5} \frac{H_m J'_m}{H'_m J_m} - 1. \tag{17}$$

Deriving $\tilde{c}_k$ from (14), we can then obtain the rest of unknowns from the formulas:

$$\tilde{a}_m = (\Delta_m + 1)\tilde{c}_m + \frac{H_m}{H'_m} F_m^{(2)}, \tag{18a}$$

$$\tilde{b}_m = \frac{\nu_m}{\pi} \sum_{n=1}^{\infty} \tilde{c}_n \frac{J'_n}{J_n} \gamma_{mn}. \tag{18b}$$

Consider now the existence of the obtained solution. According to [15], the matrix equation (14) has a unique solution in the Hilbert space of sequences (l_2) if and only if the matrix T and the right hand side (RHS) are square summable and the determinant of the system is nonzero. The existence of matrix elements T_{mn} is ensured by asymptotic behavior of series elements in (15) versus m, n, and k:

$$\frac{J_n}{J_n'}\gamma_{nk}\gamma_{nm} = O(n^{-3}k^{-2}m^{-2}) \tag{19}$$

that follows from

$$\frac{J_n}{J_n'} = O(n^{-1}), \quad \gamma_{nk} = O(n^{-1}k^{-2}), \quad \Delta_k = O(k^0). \tag{20}$$

Accounting for (19), we see that series in (15) is absolutely convergent and its sum behaves asymptotically as follows:

$$\sum_{n=1}^{\infty} \frac{J_n}{J_n'}\gamma_{nk}\gamma_{nm} = O(k^{-2}m^{-2}).$$

Accounting for such behavior of the sum and $J_k'/J_k = O(k)$, we easily obtain that

$$T_{mk} = O(k^{-1}m^{-2}), \tag{21}$$

and namely this issue insures the square summability of T that in turn ensures existence of infinite determinant in (14). As to the RHS, we can see that F_m decays exponentially fast if we account for (7), (8). Because of that, F is square summable as well. More than that, the exponentially fast decay of the RHS ensures the same diminishing rate of the solution, viz.,

$$\tilde{a}_m, \tilde{c}_m = O((k_1 a)^m 2^{-m}/m!). \tag{22}$$

At the same time, b_m only decays as m^{-1}. This one increases significantly the computational time when deriving the inward magnetic field, but does not enlarge the computational cost for the scattered field. Finally, because of the main equation (14) is Fredholm, the condition number of truncated system does not increase with truncation number in contrast to [8, 9].

Now, having the solution to the main equation (14), we can prove the correctness of its deriving. To obtain this equation, we changed the order of summation in (11b). This procedure is correct if and only if the both series converge absolutely. Let us prove that it is so. Accounting for (22), we can see that the inner series in (11b) converges exponentially fast and hence absolutely. Accounting further for (20), we can see that for large n

$$\frac{J_n}{J_n'}\sum_{k=0}^{\infty} \tilde{c}_k \frac{J_k'}{J_k}\gamma_{nk} = O(n^{-2}),$$

and then the outer series in (11b) converges absolutely as well. This one proves the correctness of deriving of the main equation (14).

Consider now the existence of the BVP solution in D^- and D^+. Prove that the scattered field in D^-

$$H_s^- = \sum_{n=0}^{\infty} \tilde{a}_n \frac{H_n^{(2)}(k\rho)}{H_n^{(2)}(ka)} \cos n\varphi, \tag{23}$$

and the whole field in D^+

$$H^+(\rho,\varphi) = \sum_{n=1}^{\infty} \tilde{b}_n \frac{J_n(k_1\rho)}{J_n'(k_1 a)} \sin n\varphi + \sum_{n=0}^{\infty} \tilde{c}_n \frac{J_n(k_1\rho)}{J_n(k_1 a)} \cos n\varphi \tag{24}$$

exists for any ρ and φ. Really, in D^- we have $\rho > a$ and

$$\lim_{n\to\infty} H_n^{(2)}(k\rho)/H_n^{(2)}(ka) = 0.$$

Because of that, the series in (23) converges exponentially for any $\rho \geq a$ and φ if we account for (22). In D^+, $\rho < a$ and for large n we have asymptotic behaviors

$$\begin{aligned} J_n(k_1\rho)/J_n(k_1 a) &= O((\rho/a)^n), \\ J_n(k_1\rho)/J_n'(k_1 a) &= O(n^{-1}(\rho/a)^n) \end{aligned}$$

that prove the absolute convergence in (24) for any $\rho < a$ and φ. On the boundary $\rho = a$, the first series in (24) converges as n^{-2}, if we account for (18b) and (20), and the second series converges exponentially fast. Summarizing, we can affirm that proposed BVP solution exists in any point of upper half-space and on the whole infinite interface.

3. NUMERICAL FEATURES

The main issue of infinite system solving is the behavior of a truncated system solution with the truncated number (M) increasing. Fig. 2a shows the solution to the matrix equation (14) for $ka = 20$, $\varepsilon = 1$, and normal incidence. We compare herein two solutions for $M = 50$ (dotted curve) and $M = 100$ (solid curve) harmonics and demonstrate the exponentially fast decay of Fourier coefficients $\tilde{c}_m$. The coefficients $\tilde{a}_m$ have analogous decay rate. Both these coefficients derive the scattered field and ensure desirably low computational burden of numerical solution. In contrast to these two coefficients the third one, $\tilde{b}_m$, decays more slowly. Its decay rate is demonstrated in Fig. 2b. These figures show numerically the stability of a solution and its tendency

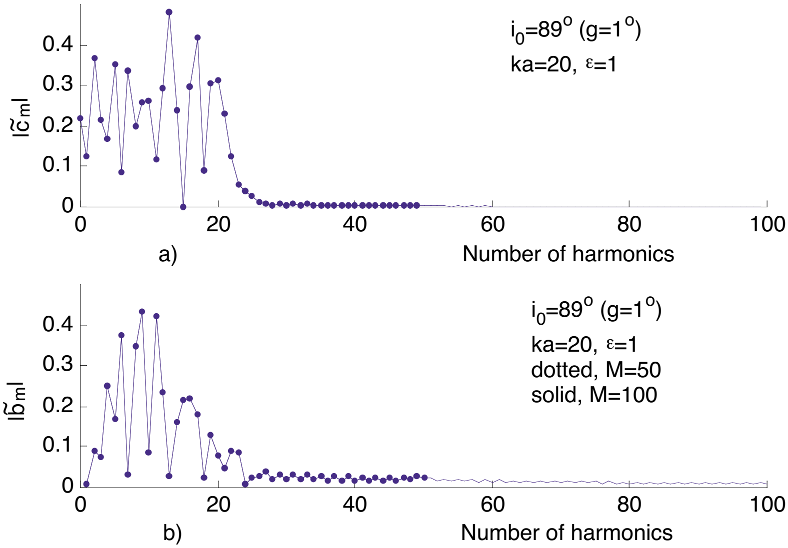

Figure 2. Solutions, $\tilde{c}_m$ and $\tilde{b}_m$, of truncated system for $M = 50$ and $M = 100$ harmonics.

to some limit, as it must be for any Fredholm-like equation. As far as the existence and uniqueness of 2-D Neumann problem considered is already proved theoretically, the adequacy of an approximate solution $\{\tilde{a}_m, \tilde{b}_m, \tilde{c}_m\}$ of a truncated system of Mth order can be confirmed only if the fields matching error on the boundary tends to zero with M increasing. The numerical confirmation that the matrix equation (14) is Fredholm is collected in Table 1 for $i_0 = 89°$, $\varepsilon = 1$, and different electric sizes (ka) of the trough. For mentioned scatterers, the following quantities are given in the table versus the truncation number (M): the relative boundary condition error on the metal semi-circle ($\rho = a,\ \pi < \varphi < 2\pi$)

$$e^{(M)} = \left\| \sum_{n=1}^{M'} \tilde{b}_n^{(M')} \sin n\varphi + \sum_{n=0}^{M} \tilde{c}_m^{(M)} \frac{J_n'}{J_n} \cos n\varphi \right\|_2 \Bigg/ \left\| \sum_{n=1}^{M'} \tilde{b}_n^{(M')} \sin n\varphi \right\|_2, \tag{25}$$

where $M' \gg M$, $\| \circ \|_2$ is the Frobenius vector-norm and $\tilde{c}_m$ is derived from (14); the Frobenius norm $n^{(M)}$ of truncated Mth-order matrix T; the condition number of truncated algebraic system $c^{(M)}$, and the dimensionless monostatic radar cross section (MRCS) for

Table 1. The main characteristics of obtained solution for $i_0 = 89°$ and $\varepsilon = 1$.

M		50	100	150	200
ka=20	$e^{(M)}$	$5.2657 \cdot 10^{-4}$	$8.0790 \cdot 10^{-5}$	$3.2912 \cdot 10^{-5}$	$1.7835 \cdot 10^{-5}$
	$n^{(M)}$	$1.4891 \cdot 10^{3}$	$1.4898 \cdot 10^{3}$	$1.4898 \cdot 10^{3}$	$1.4899 \cdot 10^{3}$
	$c^{(M)}$	$2.1455 \cdot 10^{3}$	$2.1701 \cdot 10^{3}$	$2.1809 \cdot 10^{3}$	$2.1877 \cdot 10^{3}$
	$\sigma_b^{(M)}$, dB	12.6996	12.7495	12.7562	12.7579
	t, s	1.0	2.6	6.5	12.5
M		100	150	200	250
ka=50	$e^{(M)}$	$8.5970 \cdot 10^{-4}$	$2.0526 \cdot 10^{-4}$	$8.4931 \cdot 10^{-5}$	$4.5414 \cdot 10^{-5}$
	$n^{(M)}$	278.3191	278.5644	278.7110	278.8311
	$c^{(M)}$	405	408	410	411
	$\sigma_b^{(M)}$, dB	16.6367	16.6598	16.6631	16.6632
	t, s	2.8	6.3	17.0	21.6
M		150	200	250	300
ka=100	$e^{(M)}$	0.0015	$4.3313 \cdot 10^{-4}$	$1.8489 \cdot 10^{-4}$	$9.6561 \cdot 10^{-5}$
	$n^{(M)}$	$1.0108 \cdot 10^{3}$	$1.0111 \cdot 10^{3}$	$1.0111 \cdot 10^{3}$	$1.0112 \cdot 10^{3}$
	$c^{(M)}$	$1.4940 \cdot 10^{3}$	$1.4993 \cdot 10^{3}$	$1.5039 \cdot 10^{3}$	$1.5076 \cdot 10^{3}$
	$\sigma_b^{(M)}$, dB	20.4754	20.5381	20.5635	20.5764
	t, s	7.3	13.4	23.0	36.1

backscattering

$$\sigma_b^{(M)} = \lim_{\rho\to\infty} \frac{2\pi\rho k \left|H_s^{(M)}\right|^2}{|H_0|^2}. \tag{26}$$

With the goal of comparison with [7, 9], we also calculate the backscattering width (BW)

$$\sigma_w^{(M)} = \lim_{\rho\to\infty} \frac{2\pi\rho \left|H_s^{(M)}\right|^2}{|H_0|^2} \tag{27}$$

and the far-zone scattered field amplitude

$$P_h(\varphi) = \lim_{\rho\to\infty} \sqrt{0.5\pi k\rho}\,|H_s(\rho,\varphi)|. \tag{28}$$

Finally, we note that all calculations were done in the MATLAB programming area using a PC Pentium Pro 200 MHz. While evaluating the Bessel functions of high order, we used the MATLAB codes. The correctness of these codes was controlled using the recurrent formulas giving in [16]. The MATLAB codes for Bessel functions revealed their high accuracy for any order of them. It is also confirmed by monotonous decreasing of the boundary condition error with the truncation number increasing.

4. NUMERICAL RESULTS

Despite the presented method is numerically rigorous and applicable for scatterers of any size, we compare in this section the results obtained in this paper with that of [7, 9] valid for low frequencies only with the goal of verifying our numerical algorithm. Fig. 3a shows excellent agreement of results for vacant trough of $ka = 2\pi\,(a = \lambda)$ for normal incidence ($i_0 = 0°$). For lossless dielectric loading with $\varepsilon = 3$, the agreement is rather good as well, but worse than for abovementioned vacant trough as we can see in Fig. 3b. This is due to strong resonances in dielectric cylinder that make worse the accuracy of a solution to ill-conditioned system treated in [9]. This paper solutions

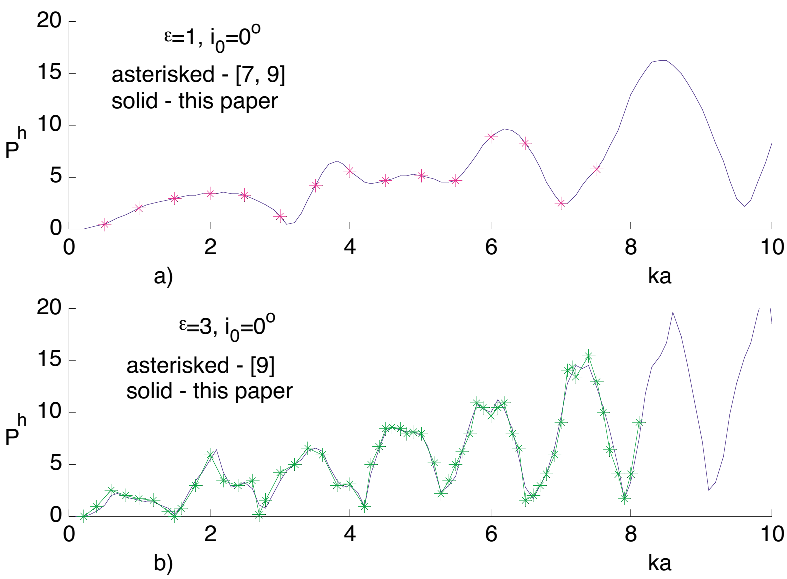

Figure 3. Far-zone scattered field amplitude, P_h, versus ka for the vacant trough, (a), and dielectric loaded trough, (b), for normal incidence ($i_0 = 0°$).

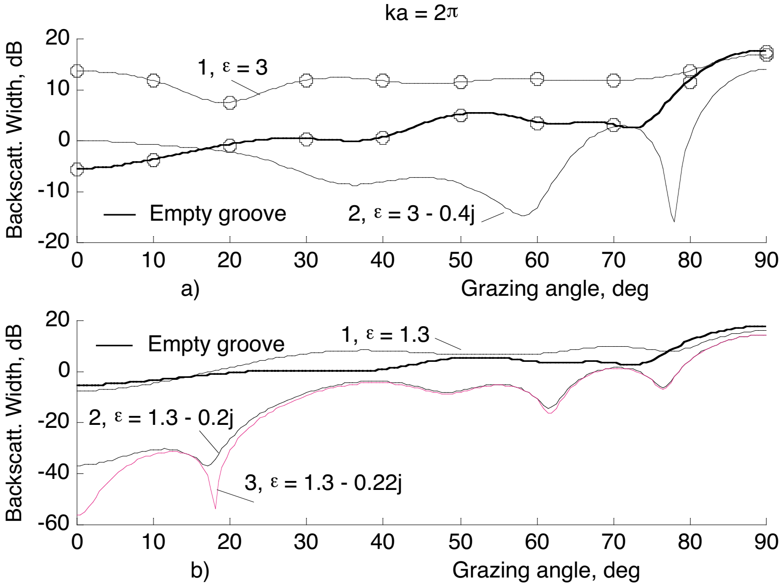

Figure 4. Backscattering width for empty and dielectric loaded grooves versus grazing angle, g, for some ε' and ε'' in the low-frequency range ($ka = 2\pi$). Circled curves correspond to [9], solid curves — to this paper.

exhibited in Fig. 3 are obtained with relative error $e^{(M)} < 10^{-4}$. The accuracy of solutions in [9] was not specified. Comparison of backscattering (BW) obtained by means of two methods, [9] and this paper, in the whole range of grazing angle $g = 90° - i_0$ is shown in Fig. 4a as circled and solid curves respectively for vacant and loaded troughs of $ka = 2\pi$ ($a = \lambda$). Excellent agreement can be noted herein as well. We can also see the enhanced backscattering for lossless dielectric loading of mentioned trough noted in [9]. However, it is worthwhile to point out that, as to author's knowledge, there are no investigations of backscatter from troughs loaded with lossy dielectric. Here, in contrast to lossless loading, the backscatter falls rapidly with increasing from zero. Its behavior for $\varepsilon'' = 0.4$ is shown in Fig. 4a (curve 2) for example considered in [9]. Strong fall-off of backscatter we can see here for any oblique incidence. Such fall-off performances depend strongly on both and as we can see in Fig. 4b for $\varepsilon' = 1.3$. The detailed investigation of this problem shows that backscatter decreases with ε'' for any ε' but to a certain value only, and then increases monotonously. The BW dependencies via are shown in Fig. 5a and 5b for the above considered

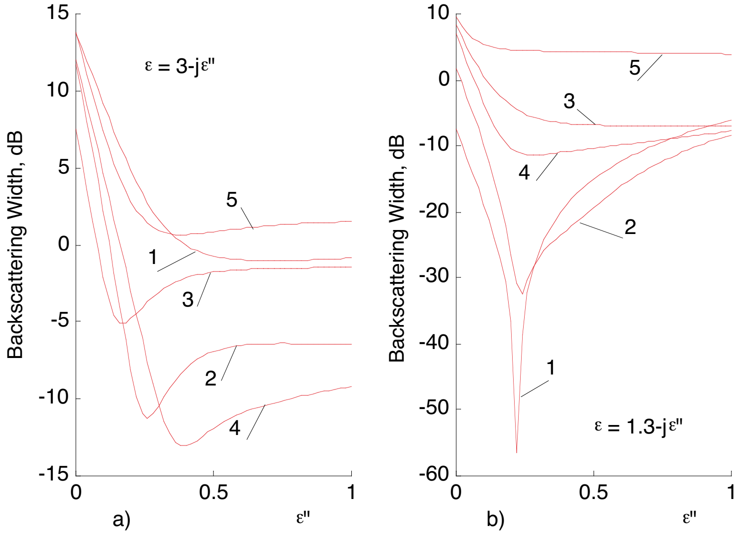

Figure 5. Extremum behavior of backscattering width versus ε'' for $\varepsilon' = 3$ and $\varepsilon' = 1.3$ in the low-frequency range.

$\varepsilon' = 3$ and $\varepsilon' = 1.3$ respectively, and for different grazing angles (0°, 20°, 40°, 60°, and 80°). These graphics show that we can pick out the parameters of loading so that a trough will be almost invisible under oblique illumination of HH radar.

Above, we consider the same trough as in [9], namely, of $ka = 2\pi\,(a = \lambda)$. In contrast to [9], we can consider troughs of any size and loading. So that, we investigate in this section the mentioned fall-off of backscattering for troughs of middle size, $ka = 100\,(a \approx 16\lambda)$ with different lossy loading. The BW behaviors for troughs loaded with dielectric of $\varepsilon = 1.3$ and $\varepsilon = 1.3 - 0.01j$ are shown in Fig. 6a, curve 1 and 2 respectively, in comparison with vacant trough (thick curve). The analogous behaviors are shown in Fig. 6b for $\varepsilon = 1.1$ and $\varepsilon = 1.1 - 0.02j$, curve 1 and 2 respectively. Here, in contrast to the low-frequency case, we can see more uniform fall-off of backscattering in the whole range of grazing angle for oblique incidence. Again, we can sort out parameters of loading so that the aperture may be almost non-scattering in back direction under oblique illumination as we can conclude from Fig. 6b (curve 2).

It is of practical interest to investigate the behavior of mentioned fall-off of backscattering versus incident field frequency or, what is the same, the electric size (ka) of a loaded trough. Corresponding backscattering characteristics are shown in Fig. 7(a)–(d) for loading

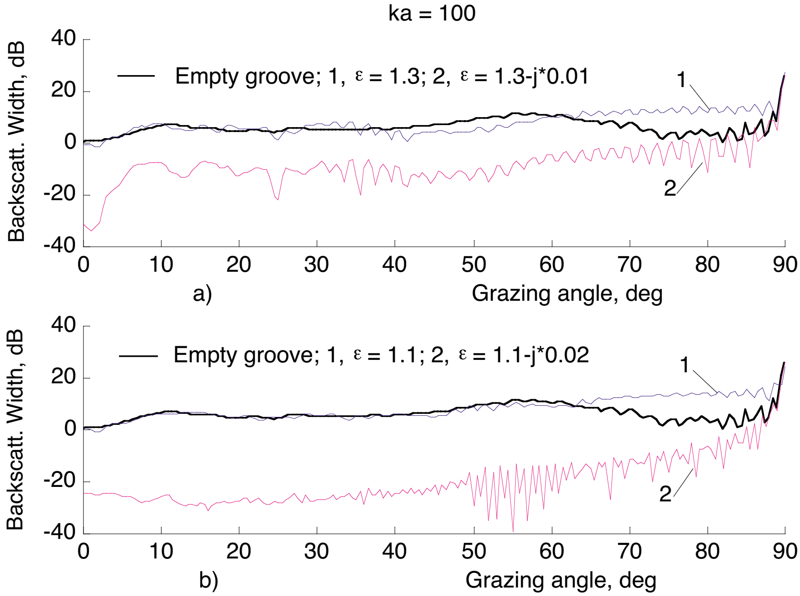

Figure 6. Backscattering width versus grazing angle for empty and dielectric loaded grooves for some ε' and ε'' in the microwave range ($ka = 100$). Fall-off of backscattering is occurred for lossy loading (curves 2) compared to lossless one (curves 1) and empty groove (thick curve).

with for grazing angles 0°, 20°, 40°, and 60° respectively (curve 2 in all figures) in comparison with backscattering from vacant trough (curve 1 in all figures). We do not show here the backscattering for ($\varepsilon = 1.1$)-loaded trough because its behavior is almost the same as that for vacant trough. These graphics show that for chosen dielectric loading the backscattering decreases significantly with frequency growth, in contrast to vacant trough, in the whole range of oblique incidence, and this effect becomes larger for larger frequencies. That is, this effect gives, theoretically, the possibility of reducing drastically the backscattering from an aperture making use of appropriate dielectric loading. More realistically, this is the first step only towards its practical implementation. Further, we plan to apply a more general method solution for scattering from rough surface with the goal of solving the mentioned problem for non-canonical geometries. The solution presented here will play, as to our opinion, a fundamental role in testing of methods that are more general.

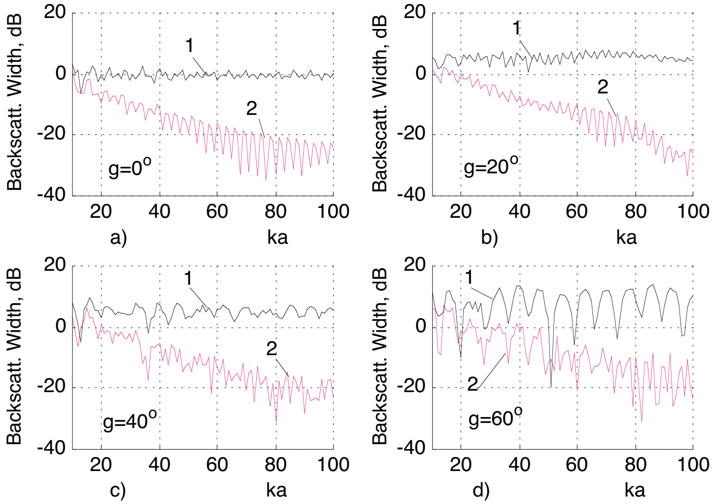

Figure 7. Backscattering width versus ka for some grazing angles ($0°$, $20°$, $40°$, $60°$) for lossy loading (curves 2) compared to the vacant trough (curves 1).

5. CONCLUSION

A new solution to the known two-dimensional canonical boundary value problem has been provided here in a rigorous manner for H-case. Coupled with analogous work for E-case [13], this paper finishes the long-time efforts to overcome this problem. Primarily, the considered BVP problem can be used for testing methods that are more general. However, some interesting scattering features have also been found from this canonical problem itself. Example is the enhanced E-scattering at low grazing for ice-loaded trough, which has been revealed in [13]. This enhanced backscattering gives a theoretical possibility of detecting an iceberg with the aid of an HH-radar at low grazing. The problem that has been solved in this paper permits one to investigate the backscattering from ice-loaded trough as well. Such investigation has been provided and revealed this opportunity to be not possible for VV remote sensing. Because of that, these results were not demonstrated in this paper for brevity. On the other hand, a strong fall-off of backscattering from lossy loaded trough has been found in this paper for V-illumination in a large range of scatterer size for oblique incidence. This effect gives a theoretical possibility to decrease drastically the backscattering from semicircular apertures under V-pol illumination.

REFERENCES

1. Harrington, R. F. and J. R Mautz, "A generalized network formulation for aperture problems," *IEEE Trans. Antennas Propagat.*, Vol. 24, 870–873, Nov. 1976.
2. Goggans, P. M. and T. H. Shumpert, "Bacscatter RCS for TE and TM exitations of dielectric-filled cavity-backed apertures in two-dimensional bodies," *IEEE Trans. Antennas Propagat.*, Vol. 39, 1224–1227, Aug. 1991.
3. Wood, Jr., W. D. and A. W. Wood, "Development and numerical solution of integral equations for electromagnetic scattering from a trough in a ground plane," *IEEE Trans. Antennas Propagat.*, Vol. 47, 1318–1322, Aug. 1999.
4. West, J. C., "On the control of edge diffraction in numerical rough surface scattering using resistive tapering," *IEEE Trans. Antennas Propagat.*, Vol. 51, 3180–3183, Nov. 2003.
5. Sachdeva, B. K. and R. A. Hurd, "Scattering by a dielectric-loaded trough in a conducting plane," *J. Applied Physics*, Vol. 48, 1473–1476, Apr. 1977.
6. Kolbehdari, M. A., H. A. Auda, and A. Z. Elsherbeni, "Scattering from a dielectric cylinder partially embedded in a perfectly conducted ground plane," *J. Electromagn. Waves Applicat.*, Vol. 3, 531–554, 1989.
7. Hinders, M. K. and A. D. Yaghjian, "Dual series solution to scattering from a semicircular channel in a ground plane," *IEEE Microwave Guided Wave Lett.*, Vol. 1, 239–242, Sept. 1991.
8. Park, T. J., H. J. Eom, W.-M. Boerner, and Y. Yamaguchi, "TM scattering froma dielectric-loaded semi-sircular trough in a conducting plane," *Trans. IEICE Commun.*, Vol. E75-B, No. 2, 87–91, 1992.
9. Park, T. J., H. J. Eom, Y. Yamaguchi, W.-M. Boerner, and S. Kozaki, "TE plane wave scattering from a dielectric-loaded semi-circular trough in a conducting plane," *J. Electromagn. Waves Applicat.*, Vol. 7, No. 2, 235–245, 1993.
10. Vardiambasis, I. O., J. L. Tsalamengas, and J. G. Fikioris, "Plane wave scattering by slots on a ground plane loaded with semicircular dielectric cylinders in case of oblique incidence and arbitrary polarization," *IEEE Trans. Antennas Propagat.*, Vol. 46, 1571–1579, Oct. 1998.
11. Scharastein, R. W. and A. M. J. Davis, "Matched asymptotic expansion for the low-frequency scattering by a semi-circular trough in a ground plane," *IEEE Trans. Antennas Propagat.*,

Vol. 48, 801–811, May 2000.

12. Tyzhnenko, A. G., "Two-dimensional scattering of H-wave from a dielectric loaded semicircular trough in a PEC ground plane," *Radiophysics and Electronics*, special issue, Vol. 7, 246–252, 2002 (in Russian).
13. Tyzhnenko, A. G., "Two-dimensional TE-plane wave scattering by a dielectric-loaded semicircular trough in a ground plane," *Electromagnetics*, Vol. 24, 357–368, July 2004.
14. Yu, J.-W., W. J. Byun, and N.-H. Myung, "Multiple scattering from two dielectric-filled semi-circular channels in a conducting plane: TM case," *IEEE Trans. Antennas Propagat.*, Vol. 50, 1250–1253, Sept. 2002.
15. Von Koch, H., "Sur un theoreme de Hilbert," *Mathem. Ann.*, Vol. 69, 266–283, 1910.
16. Strifors, H. C. and G. C. Gaunaurd, "Scattering of electromagnetic waves by a perfectly conducting cylinder with a thin lossy magnetic coating," *IEEE Trans. Antennas Propagat.*, Vol. 48, 1528–1532, Oct. 2000.

Alexander G. Tyzhnenko received the B.S. degree in radiophysics (with University Honors) and the Ph.D. degree in radiophysics (scattering in plasma medium) both from the Karkov State University, Kharkov, Ukraine, in 1969 and 1976, respectively. He has been an Associate Professor in the Department of Mathematics of the Kharkov State Economic University since 1983. His research interest is in the area of computational electromagnetics.